Desalination and Water Treatment
www.deswater.com

doi: 10.5004/dwt.2022.28077

247 (2022) 206–215
January

Eliminating the need for organic hole scavenger in the photoreduction of selenite and selenate from aqueous phase

Abdullahi Kilaco Usman[a,*] Azmi Bn Aris[a,b], Bashir Alhaji Labaran[c]

[a]*School of Civil Engineering, Universiti Teknologi Malaysia, Johor Bahru, Malaysia, email: kilacousman@graduate.utm.my (A. Kilaco Usman)*
[b]*Research Institute for Sustainable Environment, Universiti Teknologi Malaysia, Johor Bahru, Malaysia, email: azmi.aris@utm.my (A. Bn Aris)*
[c]*Civil Engineering Department, University of Hafr Al-Batin, Hafr Al-Batin, Saudi Arabia, email: labaran@uhb.edu.sa (B. Alhaji Labaran)*

Received 20 June 2021; Accepted 18 December 2021

ABSTRACT

This research work investigated the photoreduction of selenite [Se(IV)] and selenate [Se(VI)] species from the aqueous phase without the use of organic hole (h^+) scavengers. The use of organic hole scavengers to aid in photocatalytic removal of selenium species leads to the discharge of partially treated organics to water bodies which may, in turn, pose a high organic loading, leading to the utilization of the oxygen meant for aquatic lives. To achieve the said objective, ZnO/TiO_2 nanocomposite was synthesized via the sol–gel method. ZnO was immobilized on TiO_2 to increase the lifespan of excitons enough for the reduction process to complete, in the end, no organic hole scavenger is needed. The morphology, functional group, and crystal structure of the photo-catalyst were confirmed via characterization with SEM/EDS, FTIR, and XRD respectively. Photocatalytic removal of 20 ppm Se(IV)/Se(VI) were investigated at pH 4 under UV irradiation using 1 g/L ZnO/TiO_2 photo-catalyst dosage. Results obtained after 22 h irradiation show a 100% reduction of Se(VI) to the non-toxic and non-mobile form of elemental selenium. On the other hand, results obtained for the removal of 20 ppm Se(IV) show 100% oxidation of Se(IV) to Se(VI) followed by subsequent conversion of Se(VI) to elemental selenium with 79% efficiency. The results presented in this study show that complete selenite and selenate removal from the aqueous phase can be achieved through ZnO/TiO_2 photocatalysis without the use of h^+ scavengers. The photoreduction reaction kinetics were found best fitted to zeroth and first order for selenate and selenite respectively.

Keywords: Synthesis; Characterization; ZnO/TiO_2; Selenite; Selenate; Photocatalysis.

1. Introduction

Rapid industrialization and anthropogenic activities like mining, fossil fuel exploration, and agricultural activities have led to the release of various contaminants into the environment; selenium (Se) and its species are no exception [1]. Effluents from the industries contain Se in the range of 0.1–20 ppm [2]. Though selenium is an important nutrient to human and animal bodies, high concentration is toxic to their health [3]. Selenium exists in different forms ranging from organic and inorganic. The most common species of Se are 0 (elemental selenium), –2 (selenide), +4 (selenite), and +6 (selenate). Selenite (SeO_3^{2-}) and selenate (SeO_4^{2-}) are the dominant species found in contaminated

* Corresponding author.

waste streams due to their high solubility and mobility [1,3,4]. The health effect posed by the high concentration of the Se species necessitated the treatment of such contaminated wastewater. Several researchers have used TiO_2 photocatalysis to treat Se contaminated wastewater. In brief, the TiO_2 (photocatalyst), upon irradiation with UV light of energy, equals or greater than its band gap (BG) excites electrons in the Valance band (VB). These excited electrons move to the conduction band (CB), leaving behind positive holes (h^+) as in Eq. (1). The positive holes can oxidize directly or react with the hydroxyl group to form hydroxyl radicals ($OH^\bullet$).

$$TiO_2 \xrightarrow{hv} e^- + h^+ \quad (1)$$

The electrons participate in reduction by attacking an electron acceptor, for example, SeO_3^{2-} and SeO_4^{2-}. However, the high tendency of recombination of excitons (electrons and holes) either at the bulk phase or on the surface is one of the shortcomings of photocatalysis. To prevent this, the photocatalytic reduction of pollutants is usually achieved by introducing holes' scavengers. These holes' scavengers, mainly organics, are easily oxidized by the h^+ and $OH^\bullet$, leaving the electrons for reduction as illustrated in Eqs. (2) and (3).

$$\text{Oxidation: } OH^\bullet / h^+ + \text{Organics} \rightarrow \text{Intermediates} \rightarrow CO_2 + H_2O \quad (2)$$

$$\text{Reduction: } SeO_{3(aq)}^{2-} / SeO_{4(aq)}^{2-} + e^- \rightarrow Se_{(s)}^0 \quad (3)$$

Researchers have employed various organic holes' scavengers in the successful TiO_2 Photoreduction of SeO_3^{2-} and SeO_4^{2-} [1,4–20]. However, these organic hole scavengers are usually left partially treated at the end, with a concentration ranging from 123 ppm C to 300 ppm C. US EPA requires a maximum TOC discharge limit of 30 ppm C on a 30 d average. Furthermore, some of these organic hole scavengers are biodegradable [21,22] and thus, their release into water bodies may significantly deplete the dissolved oxygen level, thereby affecting aquatic lives. From the reviewed literature to date, no study was carried out to synthesize a photo-catalyst for the photoreduction of Se ions without the use of organic holes' scavengers, hence our study. In this paper, ZnO/TiO_2 was synthesized, characterized using SEM/EDS, XRD, and FT-IR techniques, and used for the photoreduction of SeO_3^{2-} and SeO_4^{2-} from aqueous phase without the use of organic holes' scavengers. Research on the optimization of the synthesis parameters is ongoing. The optimized catalyst will be used to study the factors affecting the photocatalytic reduction of the selenium species because of their vital importance in the treatment process. However, this paper aims to share our preliminary findings on the evidence for synthesizing a modified photo-catalyst capable of eliminating the use of organic holes' scavengers in the photocatalysis-based removal of selenium species from the aqueous phase.

2. Materials and methods

2.1. Materials

All chemicals used in this study are of high purity and reagent grade level. Zinc acetate dihydrate ($Zn(CH_3COO)_2 \cdot 2H_2O$, 99.8%), P25 Degussa TiO_2 (99.9%), sodium selenite (Na_2SeO_3, ALDRICH), potassium selenate ($KSeO_4$, ALDRICH), sodium carbonate (Na_2CO_3 BDH), sodium bicarbonate ($NaHCO_3$ BDH), sodium hydroxide (NaOH, LOBA chemie), and hydrochloric acid (HCl, LOBA chemie) were utilized in this study.

2.2. ZnO/TiO_2 synthesis

ZnO/TiO_2 photo-catalyst was synthesized by the sol-gel method, the procedure was adopted from Pugazhendhi [23] and modified. TiO_2 powder was oven-dried at 103°C for 3 h. Measured amounts of TiO_2 powder and zinc acetate dehydrate in a 1:1 ratio of $ZnO:TiO_2$ were dissolved in distilled water and ethanol respectively, and each stirred for 30 min at 30°C and 500 rpm. The two solutions were mixed, and the resulting pH was raised to 12.5 via droplet addition of 20 M NaOH under 500 rpm stirring speed at 30°C. The solution was stirred continuously for 18 h and then kept undisturbed for 7 h (sedimentation). The sediment was filtered, partially dried, and then washed three times with ethanol. The catalyst was then oven-dried for 15 h at 120°C. Subsequently, the photo-catalyst was placed in a desiccator for 5 min to cool down and then ground to powder using pestle and mortar. The schematic of the synthesis is as depicted in Fig. 1.

2.3. Characterization

The synthesized photo-catalyst (ZnO/TiO_2) was characterized using the SEM/EDS, FT-IR, and XRD. The structural morphology and the elemental composition of the catalyst were investigated using SEM/EDS (JEOL JSM-6610L, USA). The FT-IR Spectra was recorded at room temperature in the range of 400–4,000 cm^{-1} using Thermo Scientific Nicolet iS10 spectrometer model. The crystalline structure of the photo-catalyst was investigated using the XRD technique via Desktop XRD 2nd Gen D2 PHASER BRUKER for 2θ range of (20 to 90), 3.00 scan speed and 0.03°sampling step size, and the crystalline size was determined using Scherrer's Formula.

2.4. Photocatalysis experiment

1 L reactor was used for the photocatalysis experiments (PCE). Synthetic selenite and selenate wastewater were all prepared from the stock chemical reagents and high purity water from ELGA water purification system. A solution containing Se ions (selenite or selenate) and 1 g/L ZnO/TiO_2 photocatalyst were allowed to equilibrate in darkness for 30 min, after which the solution was irradiated with a UV Lamp (F15T8-BLB 15 W, 315–400 nm and a maximum peak of 352 nm wavelength). The experiment was allowed to run for 22 h, and samples were taken in close intervals for the first 2 h and later at high intervals. The experiment was conducted at pH 4 and an initial Se ion

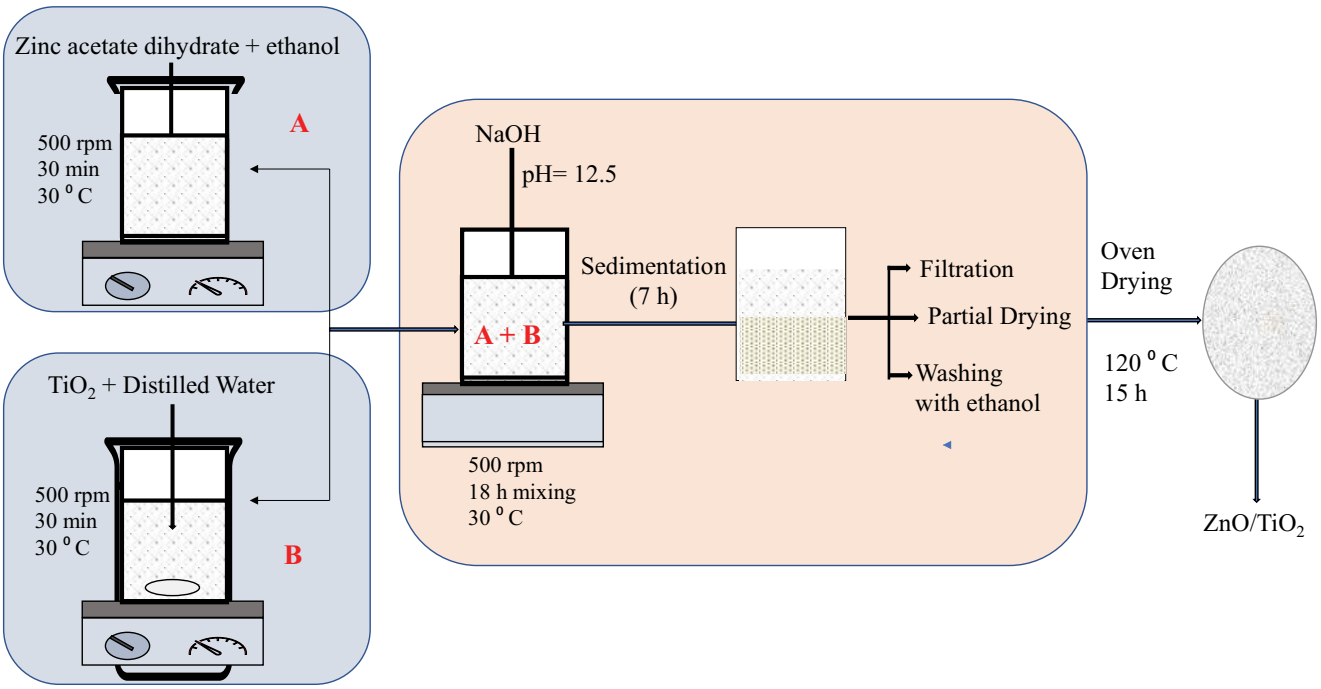

Fig. 1. Schematic of ZnO/TiO_2 nanoparticle synthesis.

concentration of 20 ppm. Fig. 2 shows the schematic of the experimental setup.

2.5. Analytical methods

Samples taken during the photocatalysis experiments were filtered using 0.2 μm membrane filters. The filtered samples were analyzed for the Se ions using an ion chromatograph set-up (Sykam Germany). The analytes were analyzed using ION A01 2.6 × 150 anion separation column and a conductivity detector. The mobile phase composition was 2.0 mM $NaHCO_3$ and 1.3 mM $NaCO_3$ with a 0.8 ml/min flow rate. Mettler Toledo (Ohio, USA) pH meter was used throughout this study for pH measurements, while pH adjustment was achieved using HCl and NaOH.

3. Results and discussion

3.1. Characterization

3.1.1. XRD analysis: crystalline structure, crystalline size, and compound identification

Fig. 3 shows the XRD pattern of the synthesized ZnO/TiO_2 hybrid, the peaks from the pattern correspond to the peaks of both ZnO and TiO_2. The presence of sharp peaks indicates the synthesized photo-catalyst to be of good crystallinity. The stick patterns in Fig. 3.1a show the peaks located at 2θ values of 25.3°, 37.8°, 48.0°, 53.9°, 55.1°, 62.7°, and 75.1°. These peaks matched the anatase form of tetragonal TiO_2 (ICSD Collection Code = 063711), with traces of rutile (ICSD Collection Code = 033844). And the stick patterns in Fig. 3.1b shows the peaks that matched hexagonal ZnO (ICSD Collection Code 067454) located at 2θ values of 37.8°, 34.4°, 36.3°, 47.5°, 56.59°, 62.9°, 67.9°, and 69.1° which were also indexed to the corresponding planes of (100), (002), (101), (102), (110), (103), (112), and (201) respectively. The results obtained herein are in good agreement with results obtainable elsewhere [23–25]. The average crystalline size of the ZnO/TiO_2 was found to be 20.02 nm using Scherrer's formula (Eq. 4)

$$D = \frac{K\lambda}{\beta\cos\theta} \tag{4}$$

where D = the size of the nanoparticle (nm), K = shape factor (0.9), λ = wavelength of the x-rays (0.1540), β = full width of θ, θ = maximum diffraction angle (radian).

3.1.2. FT-IR analysis: functional group

FT-IR analysis was carried out to determine the various functional groups on the surface of the synthesized ZnO/TiO_2 photo-catalyst. It is an essential characterization because most of the photocatalysis reaction occurs on the photo-catalyst surface. Fig. 4 shows the FT-IR spectrum for the synthesized photo-catalyst. The peaks at 420, 550.17, and 634.49 cm^{-1} are the three significant bands that confirmed the formation of the ZnO/TiO_2 hybrid. The 400–550 cm^{-1} wavenumber range is attributed to the Zn–O stretching mode of ZnO [25–29], while the 600–700 cm^{-1} wavenumber range is attributed to the vibration Ti–O–O bond [25,28,30]. The two sharp peaks at 1,018.27; 1,411.70, and 1,565.98 cm^{-1} may be attributed to the stretching of (COO^-) due to the traces of zinc acetate dehydrate used as a precursor [31]. The broad absorption peak at 3,413.73 cm^{-1}

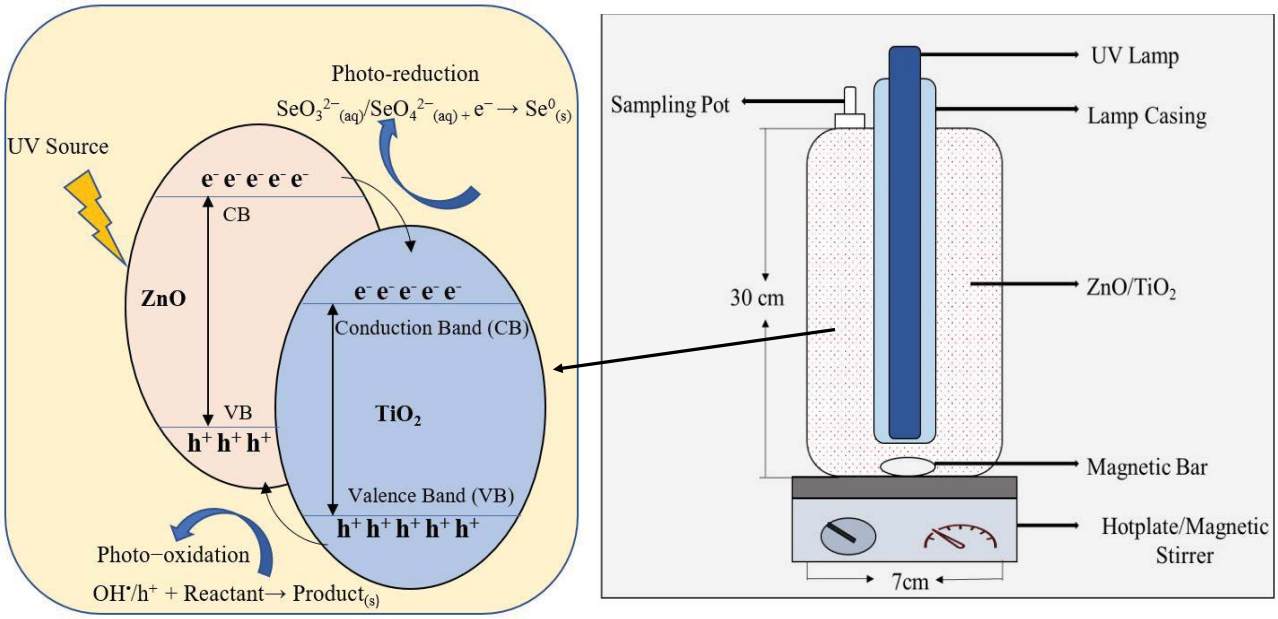

Fig. 2. Photocatalysis experimental set-up.

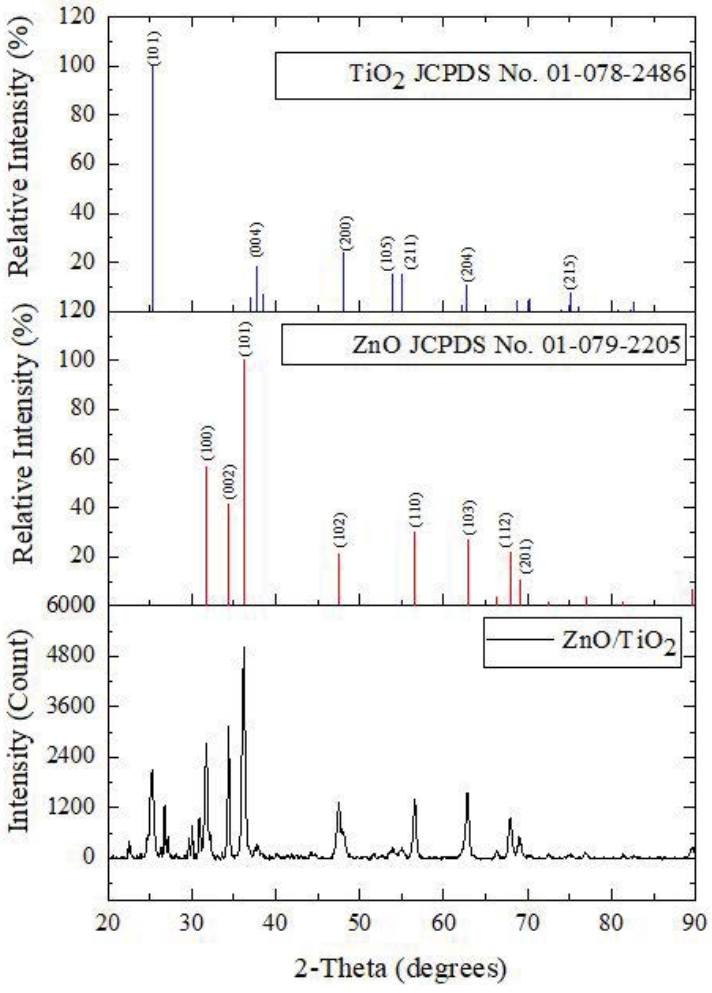

Fig. 3. XRD spectrum and peak analysis of ZnO/TiO_2 photocatalyst.

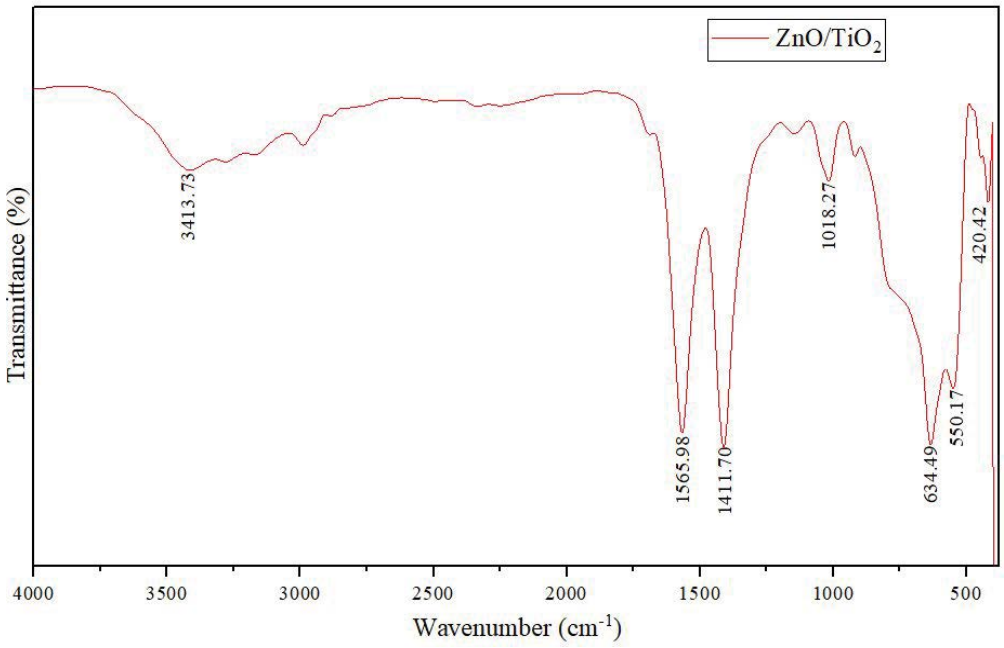

Fig. 4. FT-IR spectrum for ZnO/TiO_2 photocatalyst.

confirms the presence of –OH groups in the photo-catalyst nanostructure [25].

3.1.3. SEM/EDS analysis: morphology and elemental composition

Fig. 5 shows the SEM images from low (Fig. 5a) to high (Fig. 5f) magnification of the synthesized ZnO/TiO_2 hybrid. It can be seen that the morphology of the photo-catalyst consists of granular particles agglomerated at their boundaries. By closely looking at the higher magnified SEM pictures, it can also be seen that the particles have relatively uniform sizes. EDS spectrum was analyzed to determine the elemental composition of the ZnO/TiO_2 nanoparticle. The EDS spectrum depicted in Fig. 6 confirms the presence of zinc, titanium, and oxygen in the photocatalyst sample.

The characterization results discussed above corroborated each other in confirming the presence of ZnO and TiO_2 in the synthesized photocatalyst.

3.2. Photoreduction of selenite and selenate species

The ZnO/TiO_2 nanocomposite synthesized was tested in a 1-L reactor. The photocatalyst was suspended in the solution containing the Se ions (selenite or selenate). The gradual color change from milky white to orange-pink (Fig. 7) during the photocatalysis experiment confirms the transformation from the Se ions to elemental selenium. A control experiment with TiO_2 photocatalyst only was run for 22 h. However, no color change was noticed due to the recombination of excitons, implying no photoreduction to elemental selenium. Fig. 8a and b show the photoreduction results of the selenite and selenate, with 79% and 100% reduction efficiency to elemental selenium. The color change noticed during the PCE and results obtained from the analysis confirm the effectiveness and the promising potential of the hybrid ZnO/TiO_2 in the photoreduction of the Se ions. Coupling ZnO on TiO_2 has helped to increase the life span of the electron-hole pair enough for the reduction to occur. Studies by Johar et al. [32] corroborated this. The authors found that coupled ZnO/TiO_2 increased the lifetime of the excitons and subsequently the photocatalytic activity. Furthermore, Iqbal et al. [33] found that coupling ZnO increased the surface defects of the hybrid catalyst, thereby restraining the electron-hole pair from recombination. Another study by Jia Dong Chen et al. [34] also found that immobilizing ZnO on TiO_2 produced a hybrid catalyst, which significantly increased the separation efficiency and lifespan of the excitons.

Fig. 8a shows the photocatalysis trend for the removal of selenite from the aqueous phase. Oxidation of selenite to selenate was first observed, followed by subsequent reduction to elemental selenium. Adsorption of selenite onto the catalyst surface favors its reaction with the h^+ positioned on the catalyst's surface and the adsorbed $OH^\bullet$ leading to the oxidation of selenite to selenate. However, the selenate may desorb from the surface due to its low adsorption leading to its reaction with the excited electrons for subsequent reduction to elemental selenium. Fig. 8b shows the trend for the photoreduction of 20 ppm selenate. It should be noted that there was a direct reduction to elemental selenium and very low adsorption onto the photocatalyst surface. Low selenate adsorption onto the photo-catalyst compared to selenite may be attributed to the electrostatic bonding in selenate against the more stable ionic/covalent bonds associated with the selenite species [35]. The direct photoreduction of selenate to elemental selenium may be due to its low adsorption onto the ZnO/TiO_2 surface as explained earlier. This leads to direct contact with the excited electrons, which directly reduce it to elemental selenium.

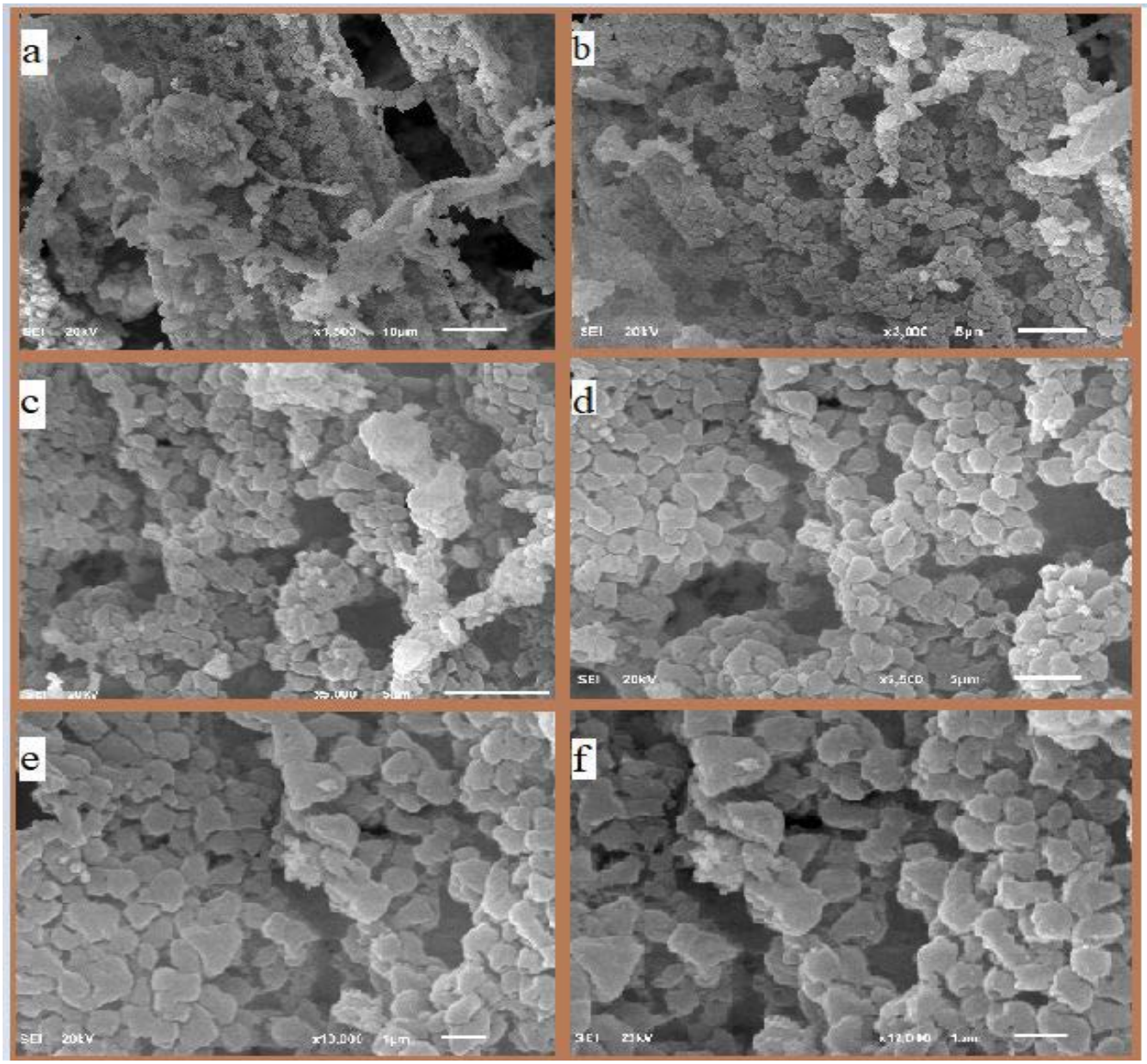

Fig. 5. SEM Micrograph of ZnO/TiO_2 photocatalyst.

3.3. Reaction kinetics of the ZnO/TiO_2 photoreduction of selenite and selenate

The kinetics of the photocatalytic reaction is an important parameter that determines how fast the reaction proceeds. It also gives information on whether the reaction is dependent or independent of the concentration of the reactants. Thus, the photoreduction experimental data for both selenite and selenate were fitted to zero-, first- and second-order kinetic models as depicted in Fig. 9. Plots in Fig. 9b(i–iii) reveal the first-order kinetic model as the best fit for selenite photoreduction with a rate constant of 0.0155 min^{-1} and an R^2 value of 0.9796. The first-order found best fitted for the selenite removal implies that the reaction rate depends on the selenite concentration. Moreover, Fig. 8a shows that selenite is first absorbed on the photo-catalyst surface before its oxidation to selenate, followed by the reduction of the selenate to elemental selenium. Selenite adsorption depends on the limited adsorption sites on the photo-catalyst surface, hence the dependence of selenite photocatalytic removal on its concentration. In contrast, the zero-order model was the best fit for the removal of selenate with a rate constant of 0.0545 ppm min^{-1} as depicted by the highest R^2 value of 0.9927. The zero-order found best fitted for the selenate photoreduction implies that a change in concentration does not affect the reaction rate. Furthermore, Fig. 8b shows that photocatalytic removal of selenate proceeds with minimal adsorption on the limited adsorption sites,

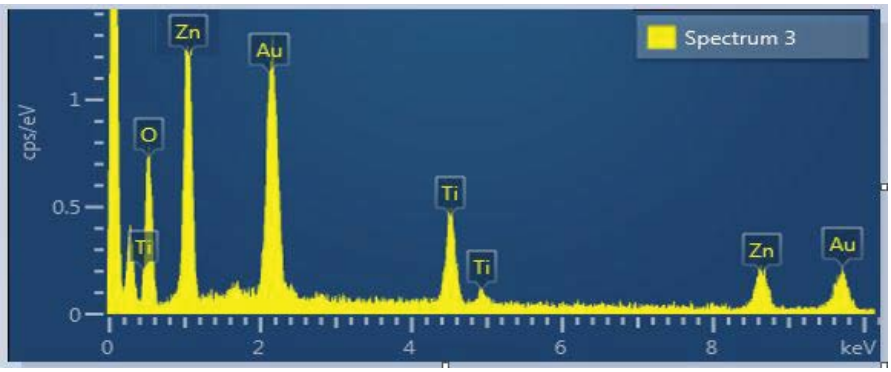

Fig. 6. EDS spectrum of ZnO/TiO_2 photocatalyst.

Fig. 7. Gradual color change during photocatalysis experiment.

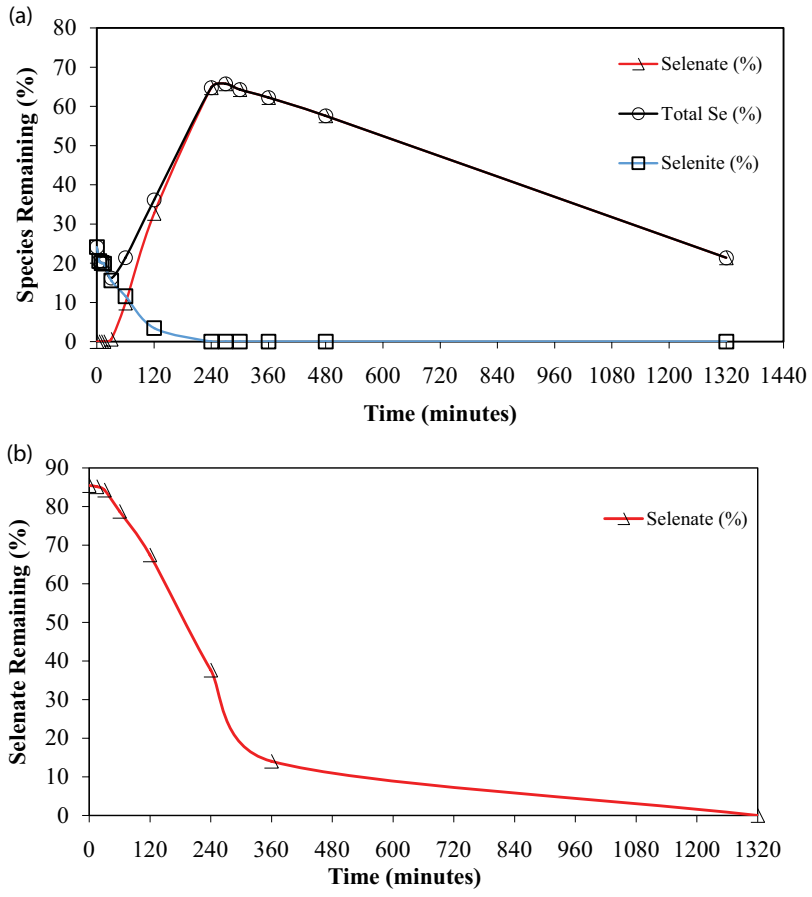

Fig. 8. Photoreduction of selenite by ZnO/TiO_2 (a) 20 ppm selenite, pH 4 and (b) 20 ppm selenate, pH 4.

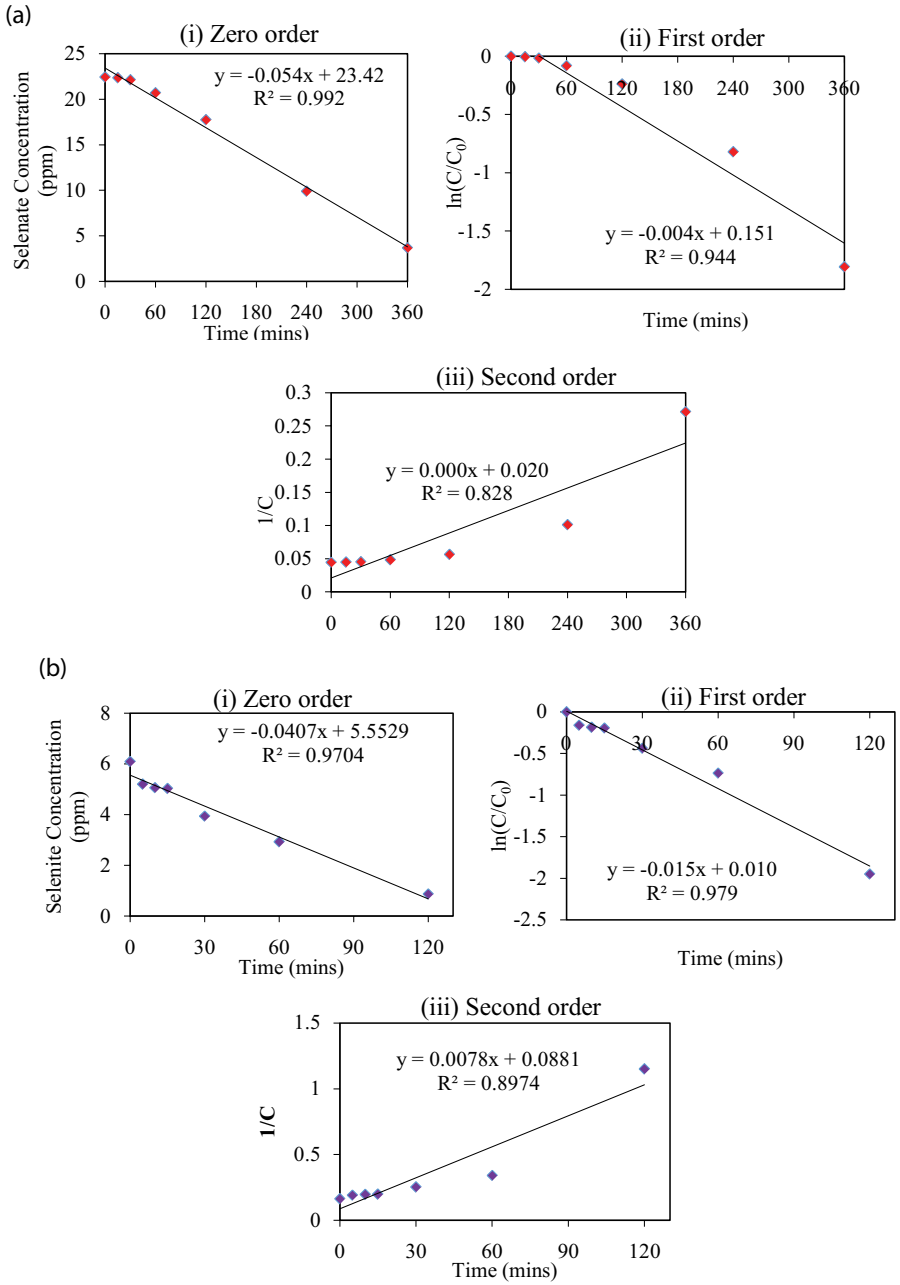

Fig. 9. Kinetic plots for the photoreduction of (a) Se(VI) and (b) Se(IV) from aqueous phase [Se(VI) = 20 ppm, pH = 4 ZnO/TiO_2 dose = 1 g/L].

and hence the lack of dependence of the removal on the concentration. It is worth noting that the zeroth and first orders found in this study are the two most common decay models observed in photocatalysis [36].

4. Conclusion

This paper carried out a study on the synthesis, characterization, and application of ZnO/TiO_2 for the photoreduction of Se ions without the use of holes scavenger; from the results and discussion, the following conclusions were drawn:

- ZnO/TiO_2 was successfully synthesized via the sol–gel technique.
- The characterization results confirmed a hybrid catalyst of hexagonal ZnO and a predominantly tetrahedral anatase TiO_2 crystal structure. The average crystalline size of the composite was calculated to be 20.02 nm. Results from EDS also confirm the presence of the composite elements (zinc, titanium, and oxygen), and a uniform morphology of agglomerated granular particles was found from the SEM micrograph.
- From the synthesized photo-catalyst and the photocatalysis experiments conducted, the results have shown

79% and 100% photoreduction of selenite and selenate to elemental selenium without the use of an organic hole scavenger. ZnO immobilization on TiO_2 was found to be responsible for extending the life span of the excitons, which made photocatalysis possible without the use of organic hole scavengers.

- For selenite, oxidation to selenate was first noticed before subsequent reduction to elemental selenium.
- The kinetic study carried out revealed the photoreduction reactions of selenate and selenite best suited for the zeroth and first-order models with rate constants of 0.0155 min^{-1} and 0.0545 ppm/min^{-1} respectively.
- It can finally be concluded that hybrid ZnO/TiO_2 photocatalysis is a potential/promising sustainable wastewater treatment technology for selenium species and other oxyanions without the use of organic holes' scavengers.

References

[1] B.A. Labaran, M.S. Vohra, Photocatalytic removal of selenite and selenate species: effect of EDTA and other process variables, Environ. Technol. (United Kingdom), 35 (2014) 1091–1100.

[2] S. Santos, G. Ungureanu, R. Boaventura, C. Botelho, Selenium contaminated waters: an overview of analytical methods, treatment options and recent advances in sorption methods, Sci. Total Environ., 521–522 (2015) 246–260.

[3] N. Geoffroy, G.P. Demopoulos, The elimination of selenium(IV) from aqueous solution by precipitation with sodium sulfide, J. Hazard. Mater., 185 (2011) 148–154.

[4] V. Nguyen, D. Beydoun, R. Amal, Photocatalytic reduction of selenite and selenate using TiO_2 photo-catalyst, J. Photochem. Photobiol., A, 171 (2005) 113–120.

[5] S. Sanuki, K. Shako, S. Nagaoka, H. Majima, Photocatalytic reduction of Se ions using suspended anatase powders, Mater. Trans., JIM, 41 (2000) 799–805.

[6] T. Tan, D. Beydoun, R. Amal, Effects of organic hole scavengers on the photocatalytic reduction of selenium anions, J. Photochem. Photobiol., A, 159 (2003) 273–280.

[7] T.T.Y. Tan, C.K. Yip, D. Beydoun, R. Amal, Effects of nano-Ag particles loading on TiO_2 photocatalytic reduction of selenate ions, Chem. Eng. J., 95 (2003) 179–186.

[8] V.N.H. Nguyen, R. Amal, D. Beydoun, Photocatalytic reduction of seleniumions using different TiO_2 photocatalysts, Chem. Eng. Sci., 60 (2005) 5759–5769.

[9] N. Aman, T. Mishra, J. Hait, R. Jana, Simultaneous photoreductive removal of copper(II) and selenium(IV) under visible light over spherical binary oxide photocatalyst, J. Hazard. Mater., 186 (2011) 360–366.

[10] B.A. Labaran, M.S. Vohra, Solar photocatalytic removal of selenite, selenate, and selenocyanate species, CLEAN – Soil, Air, Water, 45 (2017) 1600268, doi: 10.1002/clen.201600268.

[11] K. Chalastara, F. Guo, G.P. Demopoulos, Hydrolytic Precipitation of Nanosized TiO_2 Phases for Use as Photocatalytic Sorption Media in Effluent Treatment, Springer International Publishing, Cham, 2018.

[12] E. Kikuchi, S. Ito, M. Kobayashi, H. Sakamoto, Reduction and removal of selenate ion by TiO_2 photo-catalyst; Sanka chitan hikarishokubai ni yoru serensan ion no kangen jokyo, Shigen to Kankyo, 6 (1997) 71–75.

[13] E. Kikuchi, H. Sakamoto, Kinetics of the reduction reaction of selenate ions by TiO_2 photocatalyst, J. Electrochem. Soc., 147 (2000) 4589–4593.

[14] T.T. Tan, M. Zaw, D. Beydoun, R. Amal, The formation of nanosized selenium–titanium dioxide composite semiconductors by photocatalysis, J. Nanopart. Res., 4 (2002) 541–552.

[15] T.T. Tan, D. Beydoun, R. Amal, Photocatalytic reduction of Se(VI) in aqueous solutions in UV/TiO_2 system: importance of optimum ratio of reactants on TiO_2 surface, J. Mol. Catal. A: Chem., 202 (2003) 73–85.

[16] T.T.Y. Tan, D. Beydoun, R. Amal, Photocatalytic reduction of Se(VI) in aqueous solutions in UV/TiO_2 system: kinetic modeling and reaction mechanism, J. Phys. Chem. B, 107 (2003) 4296–4303.

[17] T. Nakajima, H. Takanashi, T. Tominaga, K. Yamada, A. Ohki, Removal of arsenic and selenium compounds from aqueous media by using TiO_2 photocatalytic reaction, Water Supply, 12 (2012) 24–30.

[18] M.S. Vohra, Selenocyanate ($SeCN^-$) contaminated wastewater treatment using TiO_2 photocatalysis: $SeCN^-$ complex destruction,intermediates formation, and removal of selenium species, Fresenius Environ. Bull., 24 (2015) 1108–1118.

[19] M.S. Vohra, B.A. Labaran, Photocatalytic treatment of mixed selenocyanate and phenol streams: Process modeling, optimization, and kinetics, Environ. Prog. Sustainable Energy, 39 (2020) e13401.

[20] S.A. Ahmed, M.S. Vohra, Treatment of aqueous selenocyanate ($SeCN^-$) using combined TiO_2 photocatalysis and 2-line ferrihydrite adsorption, Desal. Water Treat., 211 (2021) 267–279.

[21] J. Novak, C.D. Goldsmith, R.E. Benoit, J.H. O'Brien, Biodegradation of methanol and tertiary butyl alcohol in subsurface systems, Water Sci. Technol., 17 (1985) 71–85.

[22] C.E. Schaefer, Aerobic biodegradation of iso-butanol and ethanol and their relative effects on BTEX biodegradation in aquifer materials, Chemosphere, 81 (2010) 1104–1110.

[23] K. Pugazhendhi, S. D'Almeida, P.N. Kumar, J.S.S. Mary, T. Tenkyong, D.J. Sharmila, J. Madhavan, J.M. Shyla, Hybrid TiO_2/ZnO and TiO_2/Al plasmon impregnated ZnO nanocomposite photoanodes for DSSCs: synthesis and characterisation, Mater. Res. Express, 5 (2018) 045053.

[24] L. Wang, X. Fu, Y. Han, E. Chang, H. Wu, H. Wang, K. Li, X. Qi, Preparation, characterization, and photocatalytic activity of TiO_2/ZnO nanocomposites, J. Nanomater., 2013 (2013) 321459, doi: 10.1155/2013/321459.

[25] M. Zamani, M. Rostami, M. Aghajanzadeh, H.K. Manjili, K. Rostamizadeh, H. Danafa, Mesoporous titanium dioxide@ zinc oxide–graphene oxide nanocarriers for colon-specific drug delivery, J. Mater. Sci., 53 (2018) 1634–1645.

[26] X.Q. Wei, Z.G. Zhang, M. Liu, C.S. Chen, G. Sun, C.S. Xue, H.Z. Zhuang, B.Y. Man, Annealing effect on the microstructure and photoluminescence of ZnO thin films, Mater. Chem. Phys., 101 (2007) 285–290.

[27] S.H. Khan, R. Suriyaprabha, B. Pathak, M.H. Fulekar, Photocatalytic degradation of organophosphate pesticides (*Chlorpyrifos*) using synthesized zinc oxide nanoparticle by membrane filtration reactor under UV irradiation, Front. Nanosci. Nanotechnol., 1 (2015) 23–27.

[28] M. Naimi-Joubani, M. Shirzad-Siboni, J. Yang, M. Gholami, M. Farzadkia, Photocatalytic reduction of hexavalent chromium with illuminated ZnO/TiO_2 composite, J. Ind. Eng. Chem., 22 (2015) 317–323.

[29] I.K.R. Laila, N. Mufti, S. Maryam, A. Fuad, A. Taufiq, Sunaryono, Synthesis and Characterization of ZnO Nanorods by Hydrothermal Methods and its Application on Perovskite Solar Cells, Journal of Physics: Conference Series, The 2017 International Conference on Mathematics, Science, and Education 29–30 August 2017, Malang, East Java, Indonesia, 2018, p. 012012.

[30] M.M. Karkare, Choice of precursor not affecting the size of anatase TiO_2 nanoparticles but affecting morphology under broader view, Int. Nano Lett., 4 (2014) 111, doi: 10.1007/s40089-014-0111-x.

[31] B.H. Soni, M.P. Deshpande, S.V. Bhatt, N. Garg, S.H. Chaki, Studies on ZnO nanorods synthesized by hydrothermal method and their characterization, J. Nano- Electron. Phys., 4 (2013) 04077–04078.

[32] M.A. Johar, R.A. Afzal, A.A. Alazba, U. Manzoor, Photocatalysis and Bandgap Engineering Using ZnO Nanocomposites, Adv. Mater. Sci. Eng., 2015 (2015) 934587, doi: 10.1155/2015/934587.

[33] A. Iqbal, N.H. Ibrahim, N.R. Abdul Rahman, K.A. Saharudin, F. Adam, S. Sreekantan, R.M. Yusop, N.F. Jaafar, L.D. Wilson,

ZnO surface doping to enhance the photocatalytic activity of lithium titanate/TiO_2 for Methylene blue photodegradation under visible light irradiation, Surfaces, 3 (2020) 301–318.
[34] J. Chen, W. Liao, Y. Jiang, D. Yu, M. Zou, H. Zhu, M. Zhang, M. Du, Facile fabrication of ZnO/TiO_2 heterogeneous nanofibres and their photocatalytic behaviour and mechanism towards Rhodamine B, Nanomater. Nanotechnol., 6 (2016) 9, doi: 10.5772/62291.
[35] S. Sharmasarkar, G.F. Vance, Selenite–selenate sorption in surface coal mine environment, Adv. Environ. Res., 7 (2002) 87–95.
[36] U.I. Gaya, Kinetic Concepts of Heterogeneous Photocatalysis, in: Heterogeneous Photocatalysis Using Inorganic Semiconductor Solids, Springer, Netherlands, 2014, pp. 43–71.